Global Survey of the Relationships of Cloud Albedo and Liquid Water Path with Droplet Size Using ISCCP

QINGYUAN HAN

Department of Atmospheric Science, Global Hydrology and Climate Center, University of Alabama in Huntsville, Huntsville, Alabama

WILLIAM B. ROSSOW

NASA/Goddard Institute for Space Studies, New York, New York

JOYCE CHOU AND RONALD M. WELCH

Department of Atmospheric Science, Global Hydrology and Climate Center, Huntsville, Alabama

(Manuscript received 28 April 1997, in final form 1 August 1997)

ABSTRACT

The most common approach used to model the aerosol indirect effect on clouds holds the cloud liquid water path constant. In this case, increasing aerosol concentration increases cloud droplet concentration, decreases cloud droplet size, and increases cloud albedo. The expected decrease in cloud droplet size associated with larger aerosol concentrations has been found to be larger over land than over water and larger in the Northern than in the Southern Hemisphere, but the corresponding cloud albedo increase has not been found. Many previous studies have shown that cloud liquid water path varies with changing cloud droplet size, which may alter the behavior of clouds when aerosols change. This study examines the relationship between geographic and seasonal variations of cloud effective droplet size and cloud albedo, as well as cloud liquid water path, in low-level clouds using International Satellite Cloud Climatology Project data. The results show that cloud albedo increases with decreasing droplet size for most clouds over continental areas and for all optically thicker clouds, but that cloud albedo decreases with decreasing droplet size for optically thinner clouds over most oceans and the tropical rain forest regions. For almost all clouds, the liquid water path increases with increasing cloud droplet size.

1. Introduction

Among possible radiative forcings that can cause long-term climate change, the effect of changing tropospheric aerosols on cloud properties (called the aerosol indirect effect) is the most uncertain (0 to −1.5 W m^{-2}) relative to the other known forcings (IPCC 1996, 115). Most estimates assume that this forcing will be negative, though that is not necessarily so. However, even this range of uncertainty in the forcing implies such a large range of climate sensitivities, that are all consistent with the observed temperature changes responding to increasing greenhouse gas abundances, that policymaking is difficult (Schwartz and Andreae 1996).

The aerosol indirect effect refers to the influence of aerosols on cloud properties when they act as cloud condensation nuclei (CCN). Essentially, cloud droplets form in two nearly separate stages: a very short nucleation stage at the beginning, where cloud droplet number density increases rapidly (preexisting water-containing aerosols are ''activated''), but there is little increase in droplet size, followed by a much longer growth stage, where droplet number density remains relatively constant and droplet size increases (Rossow 1978). In the nucleation stage, cloud droplet number density is influenced by CCN concentration and updraft velocity, but in the usual case of hydrophilic CCN with a broad size distribution, the influence of CCN concentration predominates (Twomey 1977). In the droplet growth stage, droplet number density will also be altered by droplet evaporation and collision-coalescence. Thus, an increase in aerosol concentration (N_a) is expected to increase cloud droplet number density (N) and, consequently, cloud albedo (a), thereby offsetting part of the greenhouse warming (Twomey 1977; Twomey et al. 1984). Although an increase in N, by itself, would increase cloud albedo, this hypothesis usually includes the additional assumptions that the cloud liquid water content (LWC) and geometric layer thickness (h) are also constant (i.e., the cloud liquid water path, LWP = LWC × h, is constant) because they are presumed to be little

Corresponding author address: Dr. Qingyuan Han, Department of Atmospheric Science, Global Hydrology and Climate Center, University of Alabama in Huntsville, 977 Explorer Blvd., Huntsville, AL 35899.
E-mail: han@atmos.uah.edu

affected by changes in CCN concentrations. Thus, a constant LWP is widely assumed in estimating the aerosol indirect effect (e.g., Charlson et al. 1987, 1992; Slingo 1990; Jones et al. 1994; Boucher and Lohmann 1995; Jones and Slingo 1996). Based on these assumptions and the distribution of cloud optical thicknesses, a relationship between cloud albedo (at the top of the atmosphere) and cloud droplet concentration can be inferred: $\Delta\alpha \approx 0.066\Delta N/N$ for $0.3 \leq \alpha \leq 0.6$ (Twomey et al. 1984). Twomey (Twomey 1991; Platnick and Twomey 1994) later suggested an expression, $\Delta\tau/\tau = \Delta\alpha/[\alpha(1 - \alpha)] = \Delta N/(3N)$, which gives $\Delta\alpha \approx 0.08\Delta N/N$ for $0.3 < a < 0.6$. Schwartz and Slingo (1996) derived a similar relationship for albedo at cloud top, $\Delta\alpha \approx 0.075\Delta N/N$ for $0.28 < \alpha < 0.72$.

Another consequence of the assumption that LWP remains constant while N_c is increased by increasing N_a is that the mean cloud droplet radius (r) decreases. Aircraft observations have indeed shown that N_c is generally larger and r generally smaller over land than ocean (e.g., Twomey 1977), qualitatively consistent with generally larger values of N_a over land than ocean and with the assumption that LWP is about the same. The dataset of Leaitch et al. (1992) has been cited by Boucher and Lohmann (1995) and others as support for the assumption that LWP is constant even though N_c and r are changing. Satellite observations of ship tracks also focused attention on aerosol-induced changes in cloud droplet radius (Coakley et al. 1987). A satellite survey has shown that the aircraft observations are true globally: cloud droplet effective radius (r_e, see section 2) for low-level clouds is generally smaller over land than over ocean and smaller in the Northern Hemisphere than in the Southern Hemisphere (Han et al. 1994). Thus, the aerosol indirect effect has sometimes been formulated as "an increase of N_a decreases cloud droplet sizes and increases cloud albedo," but this is misleading because a reduction in droplet size by itself will, in fact, cause a decrease in scattering cross section and cloud albedo (despite the slightly larger scattering efficiency of smaller droplets). For example, for a factor of 2 change in droplet radius relative to 10 μm, the scattering cross section changes by 400%, whereas the scattering efficiency changes in the opposite direction by only about 15% (cf. Rossow et al. 1989; Nakajima et al. 1991). However, the constant LWP hypothesis predicts an overall increase in cloud albedo because the effect of increasing N_c outweighs the effect of decreasing droplet size.

The land–water and hemispheric differences of cloud droplet sizes are *qualitatively* consistent with the expected changes induced by the land–water and hemispheric differences of N_a *if* LWP is about the same. However, the corresponding hemispheric difference of cloud albedos is not found (Schwartz 1988), so LWP may not be unaffected by aerosol concentration changes. We suggested that the effect of aerosol-induced changes in cloud droplet size on cloud albedo (changed scattering cross section and scattering efficiency) might be offset by other aerosol-induced changes of cloud optical thickness (e.g., cloud droplet number density), but did not check this quantitatively (Han et al. 1994).

Since the nucleation of CCN quickly begins consuming all of the water vapor in excess of saturation in a cooling (ascending) air parcel, subsequent cloud droplet growth occurs with an approximate balance between the rates of vapor supply (continued cooling) and consumption; however, because the growth rate of the droplets increases with increasing size (surface area), the vapor supersaturation declines slowly during the growth phase. Thus, the condensation growth rate of cloud droplets is controlled by the cloud dynamics, that is, the cooling rate that determines the maximum vapor supersaturation attained, but is not directly affected by changes in N_c. The ultimate size attained by the droplets depends, therefore, on the processes that limit cloud water content; these include a finite duration of the updraft, droplet sedimentation, or the onset of collisional growth leading to precipitation (Rossow 1978).

If droplet size is limited either by the time available for growth or by sedimentation, then N_c and r are effectively independent: increasing either would increase cloud albedo, but would also increase LWP. In this case, the aerosol indirect effect would be even simpler: an increase of N_a would increase N_c producing a direct increase in albedo because cloud droplet size might remain unchanged. The albedo change in this case would be much larger than in the case of constant LWP, because there would be no offsetting decrease in albedo with decreasing droplet size. However, if there are feedbacks between the microphysical processes and the cloud dynamics, the behavior could be more complicated. Ackerman et al. (1995) argue, for example, that a reduction of cloud droplet sizes would lead to a reduction of LWC because evaporation at the cloud base stabilizes the boundary layer, decoupling the cloud from the subcloud vapor supply. Considine (1997) illustrates the effects of the decoupling by comparing two cases with different updraft velocities at cloud base: a larger updraft nucleates more droplets, leading to smaller droplets for the same LWC, but LWC is smaller at the same height above cloud base and the cloud layer is much deeper. If cloud droplet growth is limited by the onset of droplet collisions (precipitation), then the size of cloud droplets will be affected directly by changes in N_c. For the same LWC, increasing N increases the droplet collision rate (the collision rate also depends on the size dispersion), but the associated decrease in r decreases the collision rate even more (Rossow 1978); thus, because a larger value of LWC is required to attain the same precipitation efficiency, both the average LWC (as well as LWP) and the cloud lifetime are increased (e.g., Albrecht 1989). All of these theoretical considerations suggest, in fact, that LWC, and thus LWP, will not remain constant if N changes. Hence, we cannot determine how cloud albedo will change unless we also know how either LWP or cloud droplet size responds to changing aerosol concentrations.

The dataset of Leaitch et al. (1992), which is a regional composite of 92 observations from several seasons and years, is cited as support for the assumption of constant LWP. However, Nakajima et al. (1991) argue that averaging the data for different cases may hide the detailed behavior. They show, for example, that cloud optical thicknesses, τ; droplet effective radii, r_e; and LWP values, derived from four days of MCR (multispectral cloud radiometer) data during the First International Satellite Cloud Climatology Project (ISCCP) Regional Experiment (FIRE), exhibit little correlation if all of the data are averaged together; but that two different relationships appear in data for individual cases: for optically thinner clouds ($\tau \leq 15$, LWP ≤ 120 g m^{-2}), LWP and τ increase with increasing cloud droplet radius and, for thicker clouds, τ increases as r_e decreases. Rawlins and Foot (1990) found in their aircraft measurements that cloud optical thickness increases with increasing cloud droplet size. Han et al. (1994) found the same relation as Nakajima et al. (1991) in a global survey of τ and r_e for liquid water clouds obtained from 2 yr of ISCCP satellite data, with the turning point at $\tau \approx 15$–20.

Several studies explicitly illustrate the complexity of cloud property changes with changing aerosol concentration (e.g., Hobbs et al. 1970; Fitzgerald and Spyers-Duran 1973; Dytch 1975). Measurements of clouds upwind and downwind of St. Louis on two days in 1971 showed larger cloud droplets and smaller droplet concentrations upwind than downwind, consistent with an aerosol effect; but the liquid water content behaved differently in the two cases (Fitzgerald and Spyers-Duran 1973). In one case the liquid water content downwind was only half of the upwind value, so that the downwind cloud optical thickness ($\tau \approx 11.2$) was smaller than that of the upwind clouds ($\tau \approx 15.2$), despite smaller droplets and larger droplet concentrations. In the other case, where the liquid water content is about the same downwind and upwind, the downwind optical thickness ($\tau \approx 18.0$) is larger that the upwind value ($\tau \approx 16.5$). Even ship tracks turned out to involve changes of LWC (Radke et al. 1989; King et al. 1993). Stephens (1978) summarized a range of aircraft observations of cloud droplet size distributions for different cloud types over midlatitude continents (from Carrier et al. 1967) by suggesting a monotonic relationship between τ and LWP, which implies that LWP increases with increasing r_e when LWP ≥ 50 g m^{-2}. This relationship has been used in GCM studies (e.g., Fouquart et al. 1990; del Genio et al. 1996).

Satellite observations also suggest that both cloud liquid water path and cloud droplet size change when aerosol concentration changes. Minnis et al. (1992) reported a diurnal variation of cloud liquid water content, optical thickness, and cloud droplet sizes during the FIRE experiment in July 1986. The decrease of cloud droplet size, optical thickness and cloud liquid water content from morning through late afternoon can be explained by diurnally changing wind direction bringing air from the continent with larger aerosol concentrations during the afternoon and from the ocean in the morning with smaller aerosol concentrations. Twohy et al. (1995) described observations of two stratiform clouds, one pristine and one polluted, at the same location on two different days. They found that the sulfate concentration, cloud droplet concentration, and droplet sizes in the polluted cloud compared with the pristine cloud were consistent with an aerosol effect, but that the albedo difference of these two clouds was negligible because of a smaller liquid water path in the polluted cloud.

Thus, even though the available aircraft and satellite studies show the expected changes in cloud droplet sizes that could be induced by changes in aerosol concentration, they do not appear to show the corresponding changes in cloud albedo. Moreover, many of these studies suggest that LWP might not remain constant with changes in aerosol concentration. In this study, we use our near-global, multiyear dataset of cloud optical thicknesses and droplet radii (Han et al. 1994) to quantify the direct correlation of global changes of effective droplet size (r_e) and cloud albedo. This is presented in section 4a after definitions and equations are given in section 2 and the satellite datasets and retrieval methodology are briefly described section 3. The results show two different relationships: for most continental clouds and all optically thick clouds ($\tau > 15$) over most of the world, cloud albedo increases with decreasing r_e; however, for optically thin clouds ($\tau < 15$) over oceans and tropical rain forest areas, cloud albedo decreases with decreasing r_e. To find out the underlying reason, we examine the correlation of global changes of r_e and LWP in section 4b. The results show that for clouds over most regions of the world and for all seasons, LWP decreases with decreasing r_e. Thus, a decrease of r_e does not necessarily lead to a more reflective cloud as predicted by the original hypothesis. The fact that LWP is not always constant implies that cloud dynamic feedbacks may affect the magnitude of the indirect effect of aerosols. In section 5, we summarize these results and outline a different approach to determining the effects of aerosols on clouds from observations.

2. Definitions and equations

The basic equation that links cloud effective droplet radius (r_e), LWP, and optical thickness (τ) comes from the definition of r_e (Hansen and Travis 1974):

$$\tau = \frac{3}{4}\frac{Q_{\mathrm{ext}}\mathrm{LWP}}{r_e}, \tag{1}$$

where the density of water is taken to be unity and the extinction efficiency, $Q_{\mathrm{ext}} \approx 2$ for wavelengths much

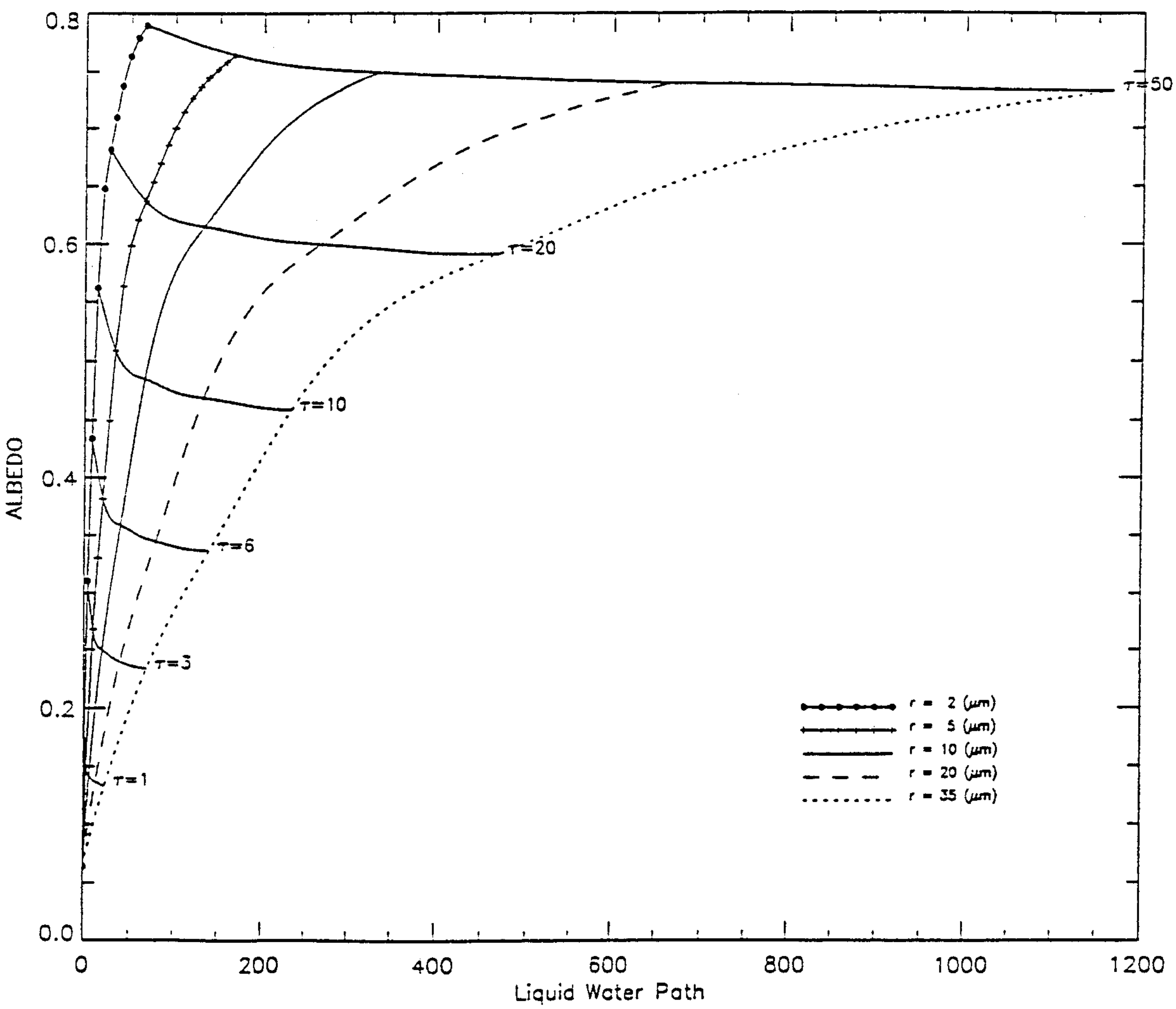

FIG. 1. Model results of cloud albedo as functions of r_e and LWP.

less than r_e. Changes in these three quantities are then related by

$$\frac{d\tau}{\tau} = \frac{d(\mathrm{LWP})}{\mathrm{LWP}} - \frac{dr_e}{r_e}. \quad (2)$$

The liquid water path can be approximated as

$$\mathrm{LWP} = \frac{4}{3}\pi r_v^3 \rho_w N h, \quad (3)$$

where water density ρ_w is unity and r_v and N_c are the volume-mean droplet radius and droplet number density, both averaged over the cloud layer of geometrical thickness, h. If the cloud droplet size distribution follows a gamma distribution (Hansen and Travis 1974),

$$n(r)\mathrm{cr}^{(1-3b)/b}e^{-(r/ab)}, \quad (4)$$

where $a = r_e$ and b is the effective variance of the size distribution, then the effective droplet size is related to the volume-mean radius by

$$r_e^3(1 - b)(1 - 2b) = r_v^3. \quad (5)$$

Aircraft measurements suggest values of b for different cloud types ranging from 0.111 for fair weather cumulus to 0.193 for stratus (Hansen 1971); thus, $r_v \approx 0.85r_e$ within about 5%. This linear relationship between r_e and r_v, also suggested by others (Martin et al. 1994; Fouquart et al. 1990), implies

$$\frac{dr_e}{r_e} \approx \frac{dr_v}{r_v}, \quad (6)$$

where we assume that b does not vary much compared with variations (at most a 15% error).

The relative variation of LWP and T can now be expressed as

$$\frac{d(\mathrm{LWP})}{\mathrm{LWP}} = 3\frac{dr_v}{r_v} + \frac{dh}{h} + \frac{dN}{N} \approx 3\frac{dr_e}{r_e} + \frac{dh}{h} + \frac{dN}{N} \quad (7)$$

and

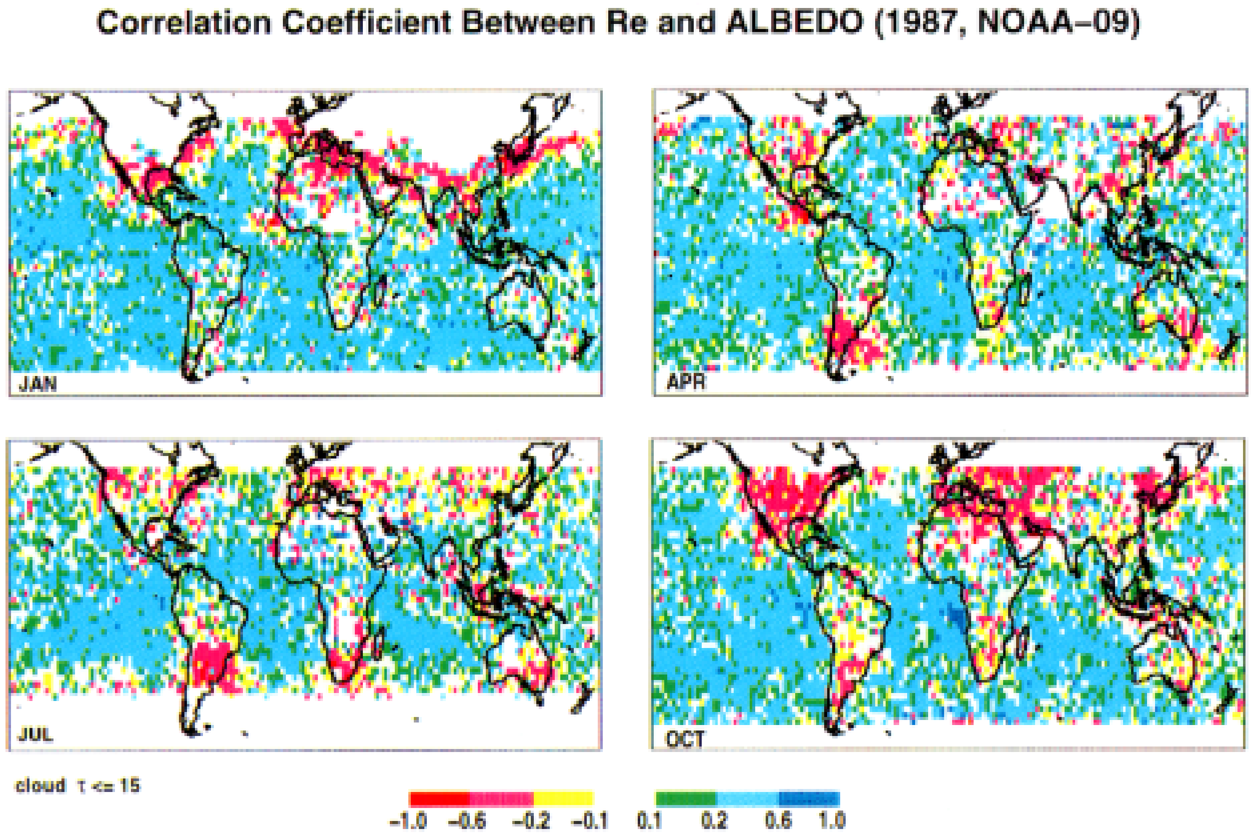

FIG. 2. Correlation coefficient between cloud effective radius and albedo of 1987 ($T \leq 15$).

$$\frac{d\tau}{\tau} = \frac{d(\mathrm{LWP})}{\mathrm{LWP}} - \frac{dr_e}{r_e} = 3\frac{dr_v}{r_v} + \frac{dh}{h} + \frac{dN}{N} - \frac{dr_e}{r_e}$$
$$\approx 2\frac{dr_e}{r_e} + \frac{dh}{h} + \frac{dN}{N}. \tag{8}$$

Since we have already averaged the droplet radius and number density over the depth of the cloud layer, we replace Nh by the mean ''column'' density, N_c. The advantage of this parameter is that it can be estimated from remote sensing data (Han et al. 1997, manuscript submitted to *Geophys. Res. Lett.*). If the cloud layer thickness is nearly constant, the relative change of N_c is the same as that of N—that is, $dN/N = dN_c/N_c$—which is usually assumed in model studies. Then the relative changes of LWP and T become

$$\frac{d(\mathrm{LWP})}{\mathrm{LWP}} = 3\frac{dr_e}{r_e} + \frac{dN_c}{N_c} \tag{9}$$

and

$$\frac{d\tau}{\tau} = 2\frac{dr_e}{r_e} + \frac{dN_c}{N_c}. \tag{10}$$

If $d(\mathrm{LWP})/\mathrm{LWP} = 0$ is assumed as in many model studies, then $dN_c/N_c = -3dr_e/r_e$ and $d\tau/\tau = -dr_e/r_e$; hence cloud optical thickness and albedo increase even though droplet size decreases. Another equivalent formulation used is that $d\tau/\tau = (1/3)dN_c/N_c$ (e.g., Platnick and Twomey 1994). If no constant LWP is assumed, and $dN_c/N_c = -\beta dr_e/r_e$ is used, then Eq. (10) implies that

$$\frac{d\tau}{\tau} = (2 - \beta)\frac{dr_e}{r_e} \tag{11}$$

so that cloud albedo will increase as long as $\beta > 2$ for $dr_e/r_e < 0$ or $\beta < 2$ for $dr_e/r_e > 0$.

3. Satellite data and retrieval method

Liquid cloud droplet sizes are retrieved by extending the ISCCP analysis of *NOAA-9* Advanced Very High Resolution Radiometer (AVHRR) data for January, April, July, and October 1985–88. The original ISCCP analysis separates cloudy and clear image pixels (area about 4 km $\times$ 1 km sampled to a spacing of about 30 km) and retrieves cloud optical thickness and top temperature (T_c) from radiances measured by AVHRR at wavelengths of 0.54–0.80 μm (channel 1) and 10.0–11.6 μm (channel 4), assuming $r_e = 10$ μm. Results for individual pixels form the ISCCP CX dataset (Rossow et al. 1991). The analysis uses the NOAA TIROS Operational Vertical Sounder (TOVS) products to spec-

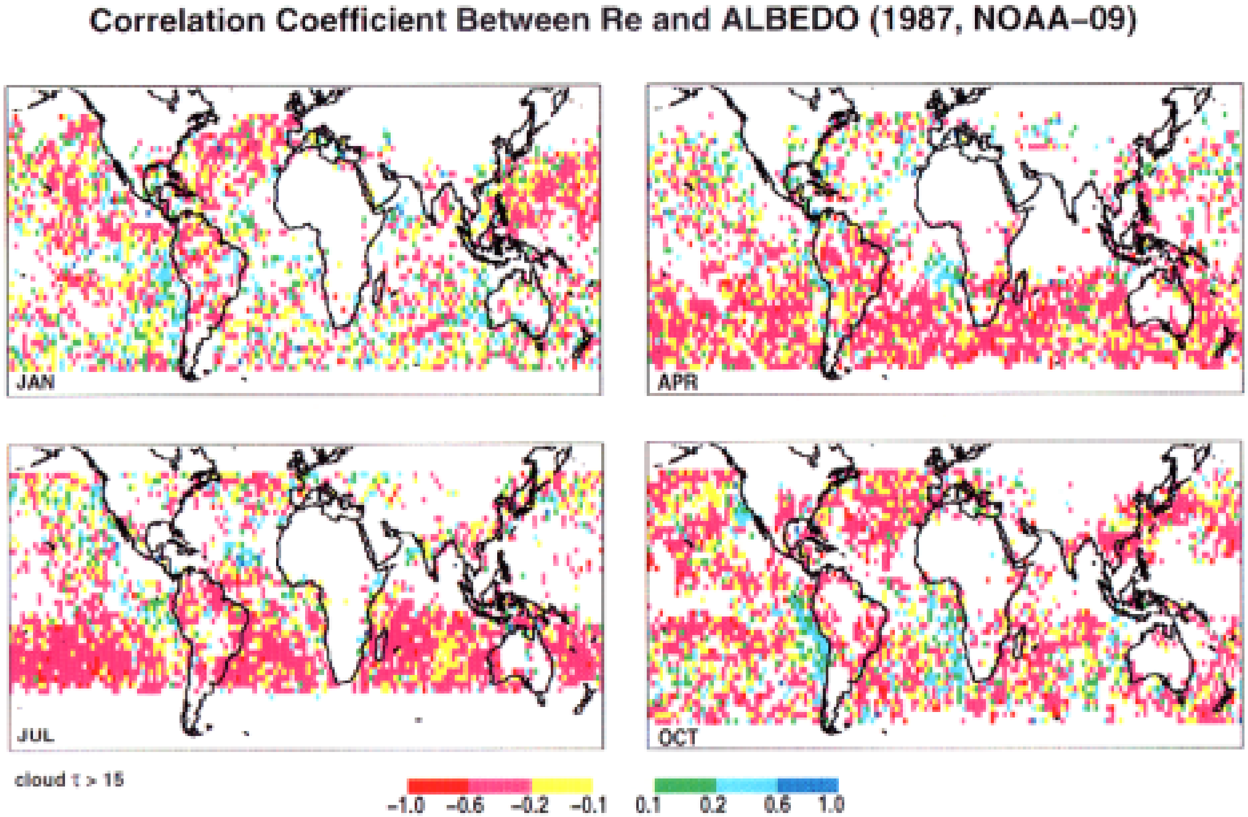

FIG. 3. Same as Fig. 2 but for $T > 15$.

ify atmospheric temperature, humidity, and ozone abundance and also retrieves the surface temperature (T_s).

The ISCCP analysis is extended by retrieving r_e from AVHRR radiances at wavelengths of 3.44–4.04 μm (channel 3) and revising the values of τ to be consistent for clouds with $T_c \geq 273$ K (Han et al. 1994, 1995). Only liquid water clouds are considered in this study because 90% of the tropospheric aerosol are distributed below 3-km altitude (Griggs 1983). Moreover, aerosol effects on ice clouds may be different than on liquid water clouds. The radiances are modeled as functions of illumination–viewing geometry by including the effects of Lambertian reflection–emission from the surface (the ocean reflectance is anisotropic, see Rossow et al. 1989); absorption–emission by H_2O, CO_2, O_3, O_2, N_2O, CH_4, and N_2 with the correlated k-distribution method (Lacis and Oinas 1991); and Rayleigh scattering by the atmosphere and Mie scattering–absorption by horizontally homogeneous cloud layers using a 12-Gauss point doubling–adding method. The droplet size distribution is assumed to the gamma distribution. Error sources are discussed and validation studies are reported in Han et al. (1994, 1995). Note that the satellite-measured radiation is sensitive only to the droplet sizes in the topmost part of the clouds; therefore, the values of LWP obtained by this analysis may be biased if r_e at cloud top is systematically different from the vertically averaged value (Nakajima et al. 1991). For nonprecipitating clouds (LWP ≤ 150 g m^{-2}), the results of this method agree well with ground-based microwave radiometer measurements (Han et al. 1995). Lin and Rossow (1994, 1996) show excellent agreement of microwave (from SSM/I) determinations of LWP over the global ocean with those obtained from the ISCCP results, assuming 10-μm droplets, and Greenwald et al. (1997) compare microwave retrievals of LWP from SSM/I and from *GOES-8* over the Pacific Ocean.

Cloud spherical albedo at 0.6-μm wavelength, calculated from the retrieved values of τ and r_e using the same radiative transfer model (including the global average effects of ozone and water vapor absorption), is used for a simple comparison of cloud effects on solar radiation. Using visible spherical albedo allows us to compare any two clouds on an equal basis, but this neglects systematic variations of reflected sunlight with solar zenith angle (latitude and time of day) and absorption of sunlight by clouds. The calculated values of cloud albedo for different combinations of r_e and LWP are shown in Fig. 1. If τ is held constant by varying N_c proportionally to r_e^{-2} [cf. Eq. (10)], a cloud with smaller r_e would have a larger albedo because of a small increase of scattering efficiency with decreased r_e (since there is no significant absorption at 0.6-μm wavelength, the scattering efficiency is indicated by Q_{ext}, which varies from 2.16 to 2.05 as r_e varies from 5 to 30 μm). If LWP is held constant by varying N_c proportionally to r_e^{-3} [cf. Eq. (9)], then cloud albedo increases as r_e decreases because τ varies proportionally to r_e^{-1}.

We look for correlated regional and seasonal variations of τ (converted to cloud albedo, α) and LWP versus variations of r_e. All of the individual pixel values are collected for each 2.5° × 2.5° map grid cell for each month, representing both spatial variations at scales ~10–100 km and daily variations over each month. A linear regression of the scattered values is used to determine correlations. Typically, about 100 samples per map grid cell per month are available; results are not reported if there are fewer than 10 samples. If, for example, ΔLWP ≈ 0, then the correlation coefficient between r_e and LWP should be approximately zero and the correlation between r_e and τ (or α) should be negative.

4. Results

a. Correlation of cloud albedo a and r_e variations

Cloud spherical albedo (α) at visible wavelengths is dependent on cloud optical thickness (or LWP) and droplet size. The global satellite survey by Han et al. (1994) confirmed results from aircraft studies (Nakajima et al. 1991) showing τ and r_e variations that are correlated differently in two ranges of τ divided at a value of about 15–20. Therefore, we examine the variations of α and r_e for these same two ranges. Figure 2 shows the correlation coefficients between a and r_e of liquid water clouds with $\tau \leq 15$ for each 2.5° × 2.5° map grid cell in January, April, July, and October 1987. Figure 3 shows the correlation coefficients for liquid water clouds with $\tau > 15$. These figures show a complicated relationship. Thinner clouds ($\tau \leq 15$) over most ocean areas and the tropical rain forests show a positive correlation between α and r_e, while over most continental areas this correlation is negative. In the former case, since α increases as r_e increases, Eq. (11) implies that $\beta < 2$; in the latter case α decreases as r_e increases with $2 < \beta < 3$. Thicker clouds ($\tau > 15$) show a negative correlation of α and r_e over most of the world with $2 < \beta < 3$. Albrecht et al. (1995) observed the same behavior in thicker marine stratus clouds during the ASTEX experiment.

Since the aerosol loading in the Northern Hemisphere is about three times larger than in the Southern Hemisphere, the usual hypothesis for the aerosol indirect effect predicts a systematically larger cloud albedo in the Northern Hemisphere; however, Schwartz (1988) showed that satellite albedo data exhibit little hemispheric albedo contrast, possibly even a higher albedo in the Southern Hemisphere. Slingo (1988) attributed this to variations of cloud amount and cloud water path between the two hemispheres that mask the effect of aerosols on cloud droplet number density and size. In addition, hemispheric differences in high-level cloud albedo (either unrelated to or differently related to aerosol changes) may further disguise the aerosol–cloud interaction in clouds at low altitudes (Langner et al. 1992; Kaufman and Nakajima 1993) where most of the aerosols are found (Griggs 1983). Our study overcomes these limitations because we isolate low-level clouds from all others, determine τ and r_e directly from observations, and calculate the cloud albedos from their properties. Since the pixel area is about 4 km^2, there is little effect of cloud cover variations within pixels [cf. Wielicki and Parker 1992, they show little change of cloud cover fraction up to a pixel size of about 1 km (note change from 2 km)] and no effect of larger-scale cloud cover on total albedo.

Figure 4 shows the zonal, annual mean values of a and r_e averaged over 1985–88 for the four months (January, April, July, and October). The values of α are calculated from the retrieved values of r_e and τ, thus, LWP $\approx \tau r_e/1.5$ [from Eq. (4)] and from Eqs. (9) and (10)

$$\frac{d(\mathrm{LWP})}{(\mathrm{LWP})} = \frac{dr_e}{r_e} + \frac{d\tau}{\tau}. \tag{12}$$

Figure 4 reveals that Northern Hemisphere clouds have smaller droplet sizes and larger albedos than Southern Hemisphere clouds for April, July, and October outside the tropical zone, qualitatively consistent with the albedo contrast expected assuming constant LWP. In the Tropics, except in October, the cloud albedos are similar in the two hemispheres. In January, α is larger in the northern subtropics but smaller in the Tropics and midlatitudes. However, Fig. 5 shows that LWP is not actually constant with latitude (or longitude): the hemispheric contrast of LWP values varies from zone to zone and season to season. Figure 6 shows values of α calculated from the same retrieved values of r_e, but assuming that LWP is fixed at its value at the equator. Comparing Figs. 4 and 6 shows that with fixed LWP the northern cloud albedos would generally be larger than the southern cloud albedos, except in the Tropics; however, LWP variations offset this effect in some latitude zones and seasons and enhance it in others. Thus, regional and interhemispheric LWP variations affect cloud albedo variations nearly as much as do variations of r_e, as Slingo (1988) cautioned.

Table 1 is a summary of cloud effective radius (r_e, in μm), LWP (in g m^{-2}), and albedo values for continental and maritime clouds in the two hemispheres, for 1988. This is a summary from about 2.8 million Global Area Coverage (GAC) pixels of AVHRR data. It shows that cloud droplet sizes and LWP of clouds in the Northern Hemisphere (NH) are both slightly smaller than those values in the Southern Hemisphere (SH). The resulting cloud albedos in the two hemispheres are almost the same as found by Schwartz (1988).

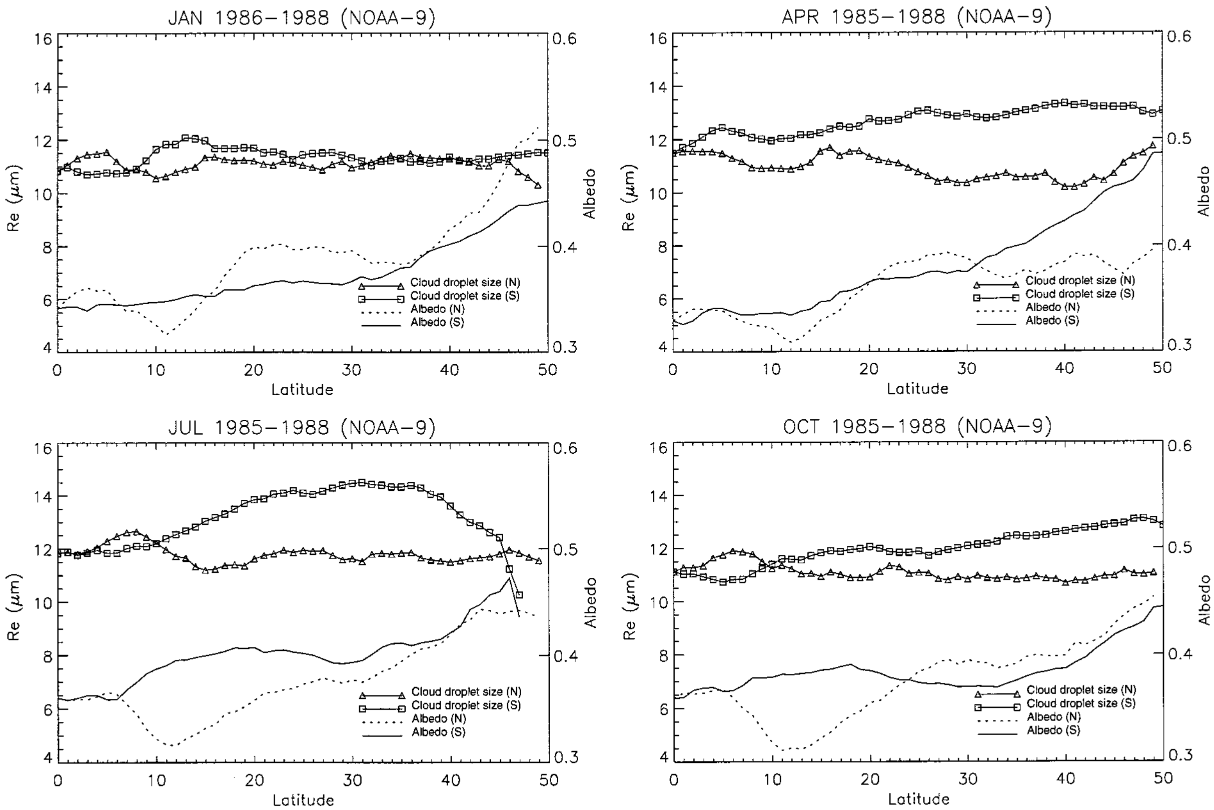

FIG. 4. Zonal distributions of retrieved r_e and cloud albedo α.

b. Correlation of cloud liquid water path and r_e variations

To clarify the role of LWP variations, we examine the correlated changes of LWP and r_e for the two ranges of cloud optical thicknesses. Figure 7 shows the correlation coefficients for each 2.5° × 2.5° map grid cell for liquid water clouds with $\tau \leq 15$ for January, April, July, and October 1987. Figure 8 shows the correlations for $\tau > 15$. The correlation of LWP and r_e is everywhere positive in all seasons, except for a few scattered locations where the correlation is negative for thicker clouds. In other words, cloud liquid water path increases with increasing r_e for all low-level clouds. The positive correlation is stronger for thinner ($\tau \leq 15$) clouds, with correlation coefficients >0.6 in most locations, than for thicker ($\tau > 15$) clouds, with correlation coefficients <0.6. This result generalizes the observations reported by Rawlins and Foot (1990), Nakajima et al. (1991), and Twohy et al. (1995) to nearly the whole globe. However, this result does not preclude the existence of clouds with larger LWP and smaller r_e, such as observed by Albrecht et al. (1995) during ASTEX experiment. Rather, it means that the large-scale variation of clouds exhibits increasing LWP with increasing r_e more often than the reverse. For thicker clouds ($\tau > 15$) in particular, the positive correlation coefficients are small (even negative in a few places), indicating that there are more chances of finding negative correlations of LWP and r_e for thicker clouds than for thinner clouds.

This result suggests that LWP may not remain constant when cloud microphysical properties are altered by changes in aerosol concentration. As we noted in the previous section, the value of β [from Eq. (11)] is generally less than three for most of the world, indicating that LWP changes may alter the effect of aerosols on cloud albedos.

5. Discussion and conclusions

The primary effect on cloud properties of changing aerosol concentrations is expected to be changes in cloud droplet number density (N_c). Thus, an anthropogenic increase in near-surface aerosol concentrations would cause an increase of N_c and, all other things remaining constant, an increase of cloud albedo. However, there is plenty of theoretical and observational evidence that the interactions of the microphysical and dynamical processes that form and destroy clouds might couple changes of N_c to changes in droplet sizes (and hence cloud water content) and to changes in vertical and horizontal extent. Lack of a comprehensive understanding of these processes has limited consideration of the aerosol effect on clouds to the case where cloud water content and vertical extent are held constant—that is, that

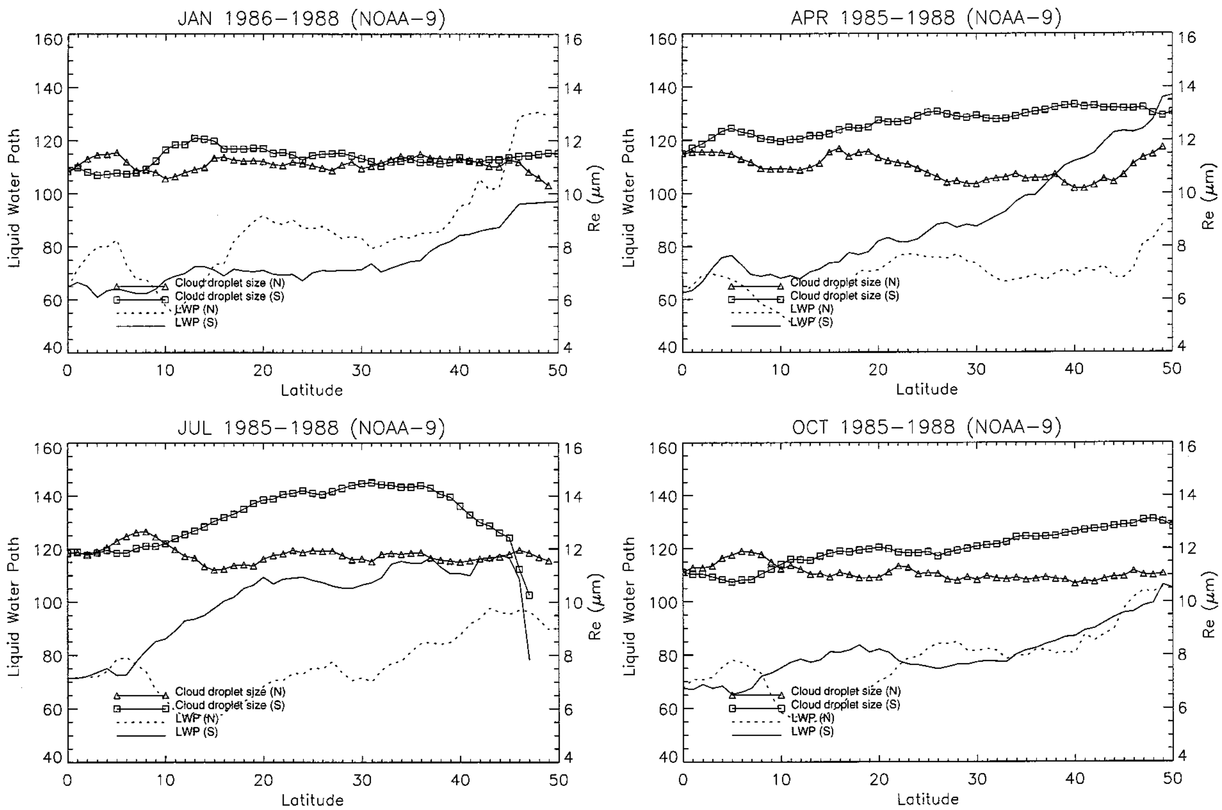

FIG. 5. Zonal distributions of retrieved r_e and cloud LWP.

cloud liquid water path is constant while N_c varies. This approach is consistent with the current state of the art in climate GCM representations of cloud processes where only cloud liquid water content and horizontal extent are determined prognostically and either N_c or r_e (or some droplet size parameter) and vertical extent are specified (e.g., Smith 1990; Tiedke 1993; Fowler et al. 1996). Notable differences are the scheme described by del Genio et al. (1996) that determines cloud vertical extent as well and the scheme described by Ghan et al. (1997) that treats the dependence of effective radius on LWC and N. To complete the cloud microphysical feedbacks in climate models, the dependence of r_e on cloud liquid water content and/or cloud droplet concentrations must be represented (Schwartz and Slingo 1996).

Large systematic differences in aerosol concentration caused by human activities and natural differences in climate are known to exist between land and ocean areas and between the Northern and Southern Hemispheres, so there have been many attempts to determine the nature of a possible aerosol effect on clouds by finding observable differences in cloud properties that could be caused by these aerosol concentration differences. Schwartz (1988) searched satellite albedo data for a systematically larger planetary albedo in the Southern Hemisphere but did not find it. However, as pointed out by Slingo (1988), this approach could have been confused by other interhemispheric differences in total cloud cover, liquid water content in low-level clouds (actually water path), and high-level cloud properties (as well as surface albedos). Since an aerosol-induced increase of N_c implies a decrease in cloud droplet radius (r_e), if LWP is approximately constant, as found in many aircraft studies, Han et al. (1994) looked for and found the expected systematic decreases of r_e over land compared with over ocean and in the Northern Hemisphere compared with the Southern Hemisphere; however, they also noticed systematic differences in cloud optical thicknesses (τ). In fact, they found that the values of τ and r_e varied together systematically, but with different relations in two regimes.

To reconcile these results, we examine the geographic and seasonal variations of cloud albedo (α) and r_e and their correlation to see what relationship appears. If LWP is constant [$d(\mathrm{LWP})/\mathrm{LWP} = 0$] while N changes, then the column number density, $N_c = Nh$, changes as $dN_c/N_c = -\beta dr_e/r_e$ with $\beta = 3$. Consequently, the cloud optical thickness varies as $d\tau/\tau = 2\, dr_e/r_e + dN_c/N_c = (2 - \beta)dr_e/r_e$, which means τ and α increase with decreasing r_e if $\beta > 2$. Our results show that this prediction is true for thicker ($\tau > 15$) clouds over oceans and all clouds over most land areas, although $2 < \beta < 3$, indicating other influences at work. However, for thinner clouds ($\tau \leq 15$) over oceans and tropical rain forests,

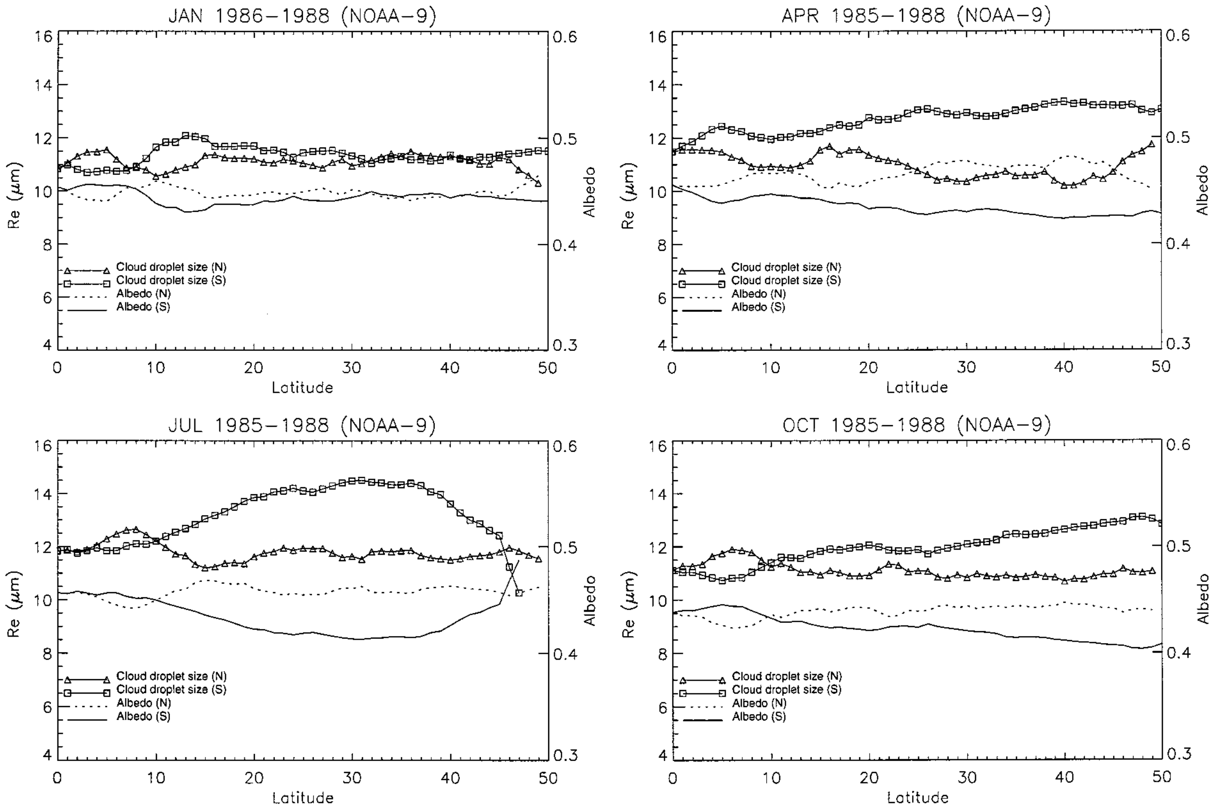

FIG. 6. Same as Fig. 4 but the cloud albedos are calculated assuming fixed LWP.

we find that τ and α decrease with decreasing r_e—that is, $\beta < 2$—contrary to the assumption that LWP is constant. The underlying reason for this more complicated behavior is that cloud liquid water generally increases with increasing r_e, which appears to overwhelm changes in N_c for optically thinner clouds.

Table 2 lists the seasonal variation and the annual mean of the percentage of thin clouds ($\tau \leq 15$) in all water clouds in 1988. This table shows more thin clouds over oceans than over land. The annual mean values show that about 79% of water clouds are thin clouds ($\tau \leq 15$) for both hemispheres. Interannual variations do not significantly change this value.

Since 79% of all low-level clouds have $\tau < 15$, the land–water and interhemispheric changes in LWP appear to dominate over possible aerosol-induced differences in N_c.

The situation is even more complicated than this summary, exhibiting regional and zonal mean differences in the relative magnitudes of the variations of τ and r_e and, consequently, differences in the variations of LWP and α. Even for most clouds over land that exhibit a correlation of α and r_e that is consistent in sign with the assumption of constant LWP, the magnitude of the difference is, in fact, altered by changing LWP values. For most clouds over ocean, except for the optically thicker clouds, the differences in LWP appear to dominate. In other words, where aerosol concentrations are already high (over land), cloud albedo and droplet size appear to vary consistently with the expectation that

TABLE 1. Hemispheric comparison of r_e, LWP, and albedo for water clouds in 1988.

		Jan			Apr			Jul			Oct			Average		
		r_e (μm)	LWP (g m^{-2})	α	r_e (μm)	LWP (g m^{-2})	α	r_e (μm)	LWP (g m^{-2})	α	r_e (μm)	LWP (g m^{-2})	α	r_e (μm)	LWP (g m^{-2})	α
NH	Land	7.8	86.8	0.46	8.4	68.6	0.43	9.4	90.9	0.46	8.0	102.7	0.48	8.5	88.4	0.46
	Ocean	12.2	97.0	0.41	12.2	84.3	0.41	12.7	92.8	0.43	11.2	92.5	0.41	12.0	92.2	0.42
	All	11.4	95.3	0.42	11.4	81.1	0.41	12.0	92.4	0.44	10.6	94.2	0.42	11.4	91.5	0.42
SH	Land	9.7	82.3	0.44	9.8	106.6	0.46	9.2	125.3	0.50	7.7	73.5	0.44	9.1	96.1	0.46
	Ocean	12.3	86.8	0.42	11.9	96.9	0.41	12.0	110.7	0.44	12.2	94.5	0.42	12.1	96.0	0.42
	All	12.1	86.4	0.42	11.7	98.0	0.42	11.7	112.2	0.45	11.9	93.1	0.42	11.9	96.0	0.42

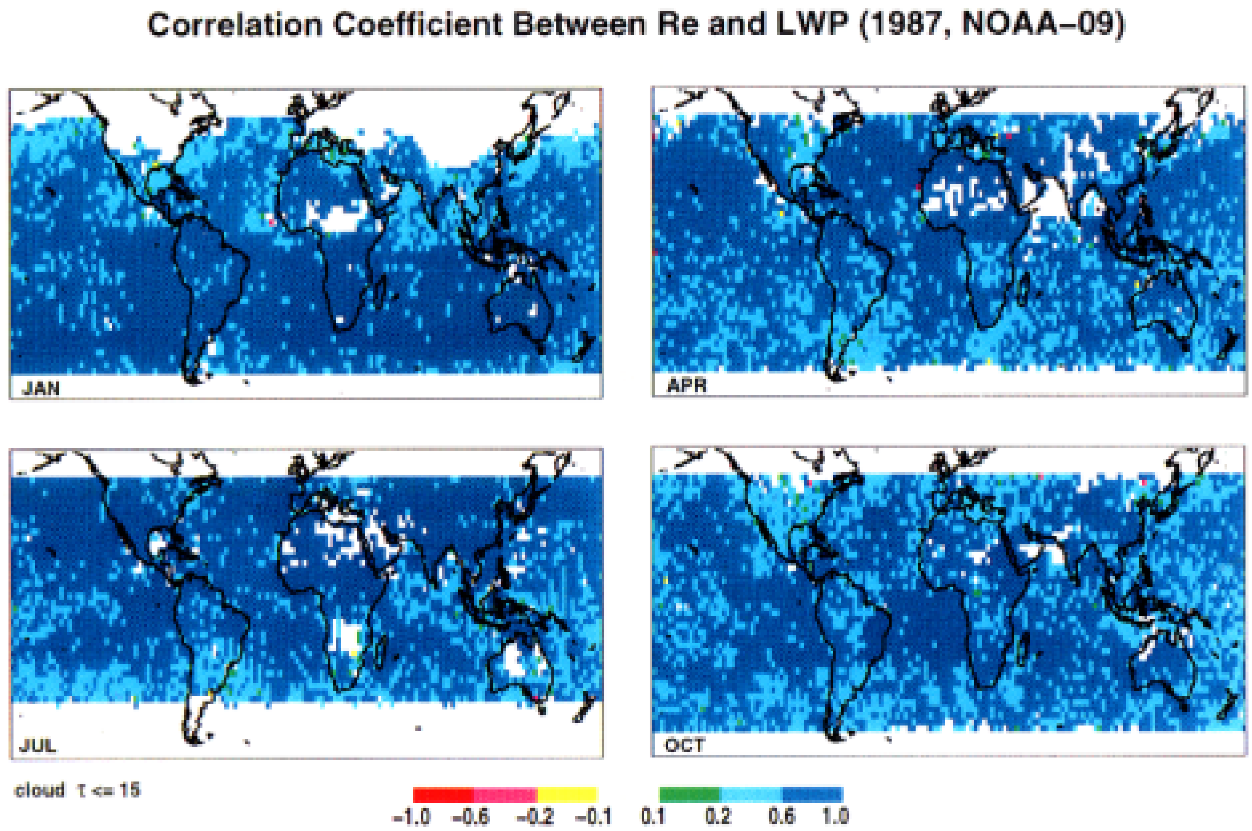

FIG. 7. Correlation coefficient between cloud efective radius and LWP of 1987 ($T \leq 15$).

LWP is approximately constant, despite some actual variation of LWP; however, where aerosol concentrations are still low (over ocean), cloud albedo and droplet size do not vary consistently with this expectation.

We have shown that the correlated variations of cloud albedo and droplet size vary with geographic (hence circulation) regime, with cloud type—optically thin or thick—and with aerosol concentration. Moreover, we have shown that these variations are not always consistent with the assumption that LWP is constant. Thus, these results are sufficient to cast doubt on previous estimates of the aerosol indirect effect by suggesting that LWP may not remain constant because cloud processes may link aerosol-induced changes in N_c to changes in other cloud properties. However, these results are not sufficient to determine what the actual effect of a systematic change in aerosol concentration would be for two reasons. First, we have determined the correlated changes of cloud properties using their day-to-day variability, which may not represent their changes under the influence of systematic aerosol changes. Second, we have not actually correlated these cloud changes with changes of aerosol concentration, rather we have shown that the correlations in day-to-day cloud property changes are different in some regions where aerosol concentrations are known to be different (however, we cannot say that aerosol concentration differences explain all of the differences in cloud behavior that we find).

TABLE 2. Percentage of thin clouds ($T \leq 15$) in total water clouds.

		Jan	Apr	Jul	Oct	Annual mean
NH	Land	74.1	81.8	76.0	68.1	74.8
	Ocean	80.2	83.3	81.2	78.1	80.4
	All	79.2	83.0	80.1	76.4	79.4
SH	Land	79.9	71.9	64.1	76.2	73.3
	Ocean	83.4	79.7	74.4	79.3	79.5
	All	83.1	78.8	73.4	79.1	79.0

As one approach to make further progress, it is necessary to derive a ‘‘column’’ cloud droplet number density that can be observed from satellites and examine its variability, together with that of droplet size, to see how this quantity varies when average aerosol concentration varies. Using a modified definition of ‘‘cloud susceptibility,’’ which is valid under the condition of changing LWP, it is necessary to compare its values for clouds over ocean and land and between clouds in the Northern and Southern Hemispheres. Finally, it is necessary to combine a method for estimating variations in aerosol column concentrations from the same AVHRR observations to compare with nearby changes

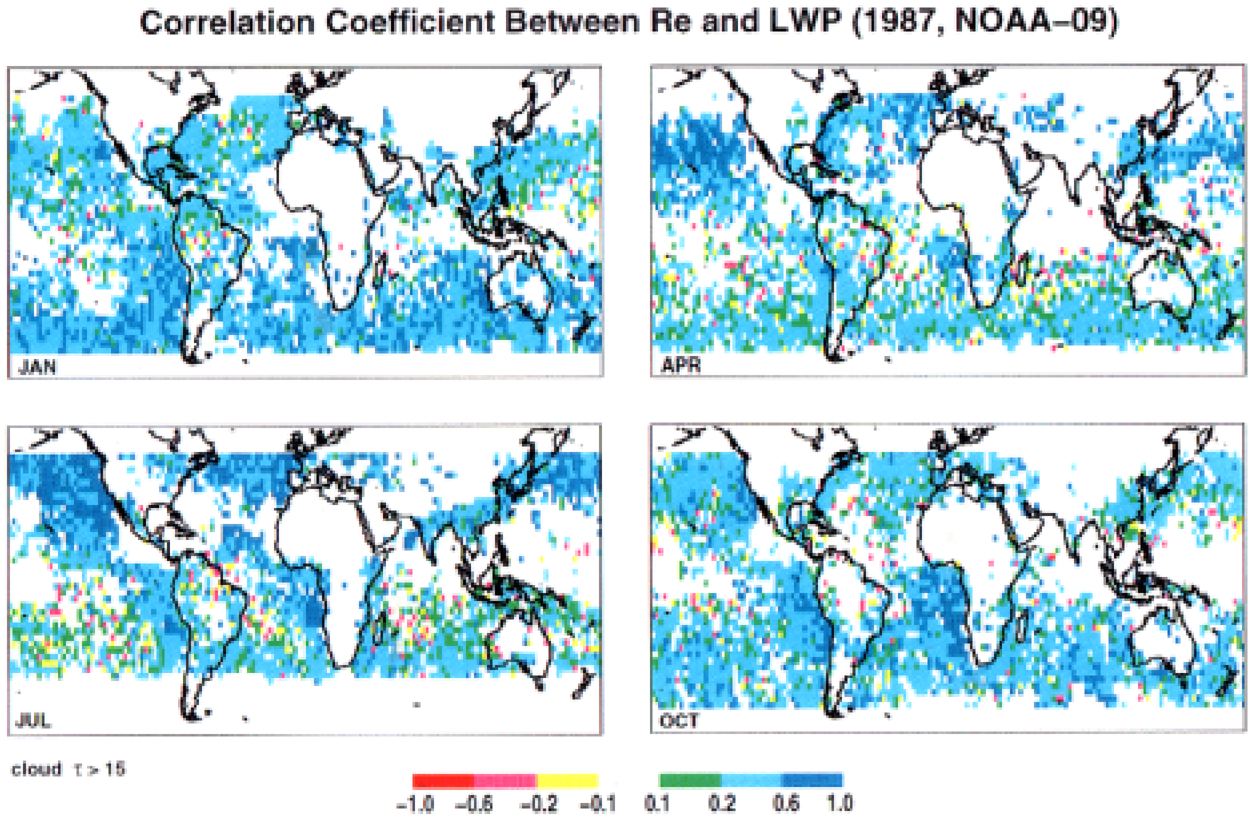

FIG. 8. Same as Fig. 7 but for $T > 15$.

in cloud droplet concentration, droplet size (and LWP), and cloud albedo. This may provide the most direct assessment of the nature of aerosol effects on clouds that is possible with today's satellite observations.

Acknowledgments. We thank two anonymous reviewers for valuable comments that helped us improve this paper. This research was supported by NASA Contract NAS1-19077 and NAG-1-542, was partially funded by the DOE NIGEC through the NIGEC GPRC (DOE Cooperative Agreement DEFC03-90ER61010). Financial support does not constitute an endorsement by DOE of the views expressed in this paper. This research was also supported by the NASA Climate Program managed by Dr. Robert J. Curran; the ISCCP international manager is Dr. Robert A. Schiffer. The ISCCP is part of the World Climate Research Program supported by the efforts of several nations.

REFERENCES

Ackerman, A. S., O. B. Toon, and P. V. Hobbs, 1995: Numerical modeling of ship tracks produced by injections of cloud condensation nuclei into marine stratiform clouds. *J. Geophys. Res.,* **100,** 7121–7133.

Albrecht, B. A., 1989: Aerosols, cloud microphysics and fractional cloudiness. *Science,* **245,** 1227–1230.

——, C. S. Bretherton, D. Johnson, W. H. Schubert, and A. S. Frisch, 1995: The Atlantic Stratocumulus Transition Experiment—ASTEX. *Bull. Amer. Meteor. Soc.,* **76,** 889–904.

Boucher, O., and U. Lohmann, 1995: The sulfate-CCN-cloud albedo effect: A sensitivity study with two general circulation models. *Tellus,* **47B,** 281–300.

Carrier, L. W., G. A. Cate, and K. J. von Essen, 1967: The backscattering and extinction of visible and IR radiation by selected major cloud models. *Appl. Opt.,* **6,** 1209–1216.

Charlson, R. J., J. E. Lovelock, M. O. Andreae, and S. G. Warren, 1987: Oceanic phytoplankton, atmospheric sulphur, cloud albedo and climate. *Nature,* **326,** 655–661.

——, S. E. Schwartz, J. M. Hales, R. D. Cess, J. A. Coakley Jr., J. E. Hansen, and D. J. Hofmann, 1992: Climate forcing by anthropogenic aerosols. *Science,* **255,** 423–430.

Coakley, J. A., R. L. Bernstein, and P. A. Durkee, 1987: Effect of ship-stack effluents on cloud reflectivity. *Science,* **237,** 1020–1022.

Considine, G., 1997: Modeling the diurnal variability in cloud microphysics in boundary layer clouds. *J. Geophys. Res.,* **102,** 1717–1726.

del Genio, A. D., M. S. Yao, W. Kovari, and K. K. W. Lo, 1996: A prognostic cloud water parameterization for global climate models. *J. Climate,* **9,** 270–304.

Dytch, H., 1975: Urban influences on cloud microstructure downwind from St. Louis, Missouri: Lower level observations. *J. Rech. Atmos.,* **9,** 145–156.

Fitzgerald, J. W., and P. A. Spyers-Duran, 1973: Changes in cloud nucleus concentration and cloud droplet size distribution associated with pollution from St. Louis. *J. Appl. Meteor.,* **12,** 511–516.

Fouquart, Y., J. C. Buriez, M. Herman, and R. S. Kandel, 1990: The influence of clouds on radiation: A climate-modeling perspective. *Rev. Geophys.,* **28,** 145–166.

Fowler, L. D., D. A. Randall, and S. A. Rutledge, 1996: Liquid and ice cloud microphysics in the CSU General Circulation Model. Part I: Model description and simulated microphysical processes. *J. Climate,* **9,** 489–529.

Ghan, S. J., L. R. Leung, R. C. Easter, and H. A. Razzak, 1997: Prediction of cloud droplet number in a general circulation model. *J. Geophys. Res.,* **102,** 21 777–21 794.

Greenwald, T. J., S. A. Christopher, and J. Chou, 1997: SSM/I and GOES-8 imager comparisons of cloud liquid water path over water: Assessment of sub-field of view effects in microwave retrievals. *J. Geophys. Res.,* **98,** 18 471–18 488.

Griggs, M., 1983: Satellite measurements of tropospheric aerosols. *Adv. Space Res.,* **2,** 109–118.

Han, Q., W. B. Rossow, and A. A. Lacis, 1994: Near-global survey of effective droplet radii in liquid water clouds using ISCCP data. *J. Climate,* **7,** 465–497.

——, ——, R. Welch, A. White, and J. Chou, 1995: Validation of satellite retrievals of cloud microphysics and liquid water path using observations from FIRE. *J. Atmos. Sci.,* **52,** 4183–4195.

Hansen, J. E., and L. D. Travis, 1974: Light scattering in planetary atmospheres. *Space Sci. Rev.,* **16,** 527–610.

Hobbs, P. V., L. F. Radke, and S. E. Shumway, 1970: Cloud condensation nuclei from industrial sources and their apparent influence on precipitation in Washington State. *J. Atmos. Sci.,* **27,** 81–89.

IPCC (Intergovernmental Panel on Climate Change), 1996: *Climate Change 1995. The Science of Climate Change.* J. T. Houghton, L. G. Meira Filho, B. A. Callander, N. Harris, A. Katenberg, and K. Maskell, Eds., Cambridge University Press, 572 pp.

Jones, A., and A. Slingo, 1996: Predicting cloud-droplet effective radius and indirect sulphate aerosol forcing using a general circulation model. *Quart. J. Roy. Meteor. Soc.,* **122,** 1573–1595.

——, D. L. Roberts, and A. Slingo, 1994: A climate model study of indirect radiative forcing by anthropogenic sulphate aerosols. *Nature,* **370,** 450–453.

Kaufman, Y. J., and T. Nakajima, 1993: Effect of Amazon smoke on cloud microphysics and albedo—Analysis from satellite imagery. *J. Appl. Meteor.,* **32,** 729–744.

King, M. D., L. F. Radke, and P. V. Hobbs, 1993: Optical properties of marine stratocumulus clouds modified by ships. *J. Geophys. Res.,* **98** (D), 2729–2739.

Lacis, A. A., and V. Oinas, 1991: A description of the correlated k-distribution method for modeling non-grey gaseous absorption, thermal emission, and multiple scattering in vertically inhomogeneous atmospheres. *J. Geophys. Res.,* **96,** 9027–9063.

Langner, J., H. Rodhe, P. J. Crutzen, and P. Zimmermann, 1992: Anthropogenic influence on the distribution of tropospheric sulphate aerosol. *Nature,* **359,** 712–716.

Leaitch, W. R., G. A. Isaac, J. W. Strapp, C. M. Banic, and H. A. Wiebe, 1992: The relationship between cloud droplet number concentrations and anthropogenic pollution: Observations and climatic implications. *J. Geophys. Res.,* **97,** 2463–2474.

Lin, B., and W. B. Rossow, 1994: Observations of cloud liquid water path over oceans: Optical and microwave remote sensing methods. *J. Geophys. Res.,* **99,** 20 907–20 927.

——, and ——, 1996: Seasonal variation of liquid and ice water path in nonprecipitating clouds over oceans. *J. Climate,* **9,** 2890–2902.

Martin, G. M., D. W. Johnson, and A. Spice, 1994: The measurement and parameterization of effective radius of droplets in warm stratocumulus clouds. *J. Atmos. Sci.,* **51,** 1823–1842.

Minnis, P., P. W. Heck, D. F. Young, C. W. Fairall, and J. B. Snider, 1992: Stratocumulus cloud properties derived from simultaneous satellite and island-based instrumentation during FIRE. *J. Appl Meteor.,* **31,** 317–339.

Nakajima, T., M. D. King, and J. D. Spinhirne, 1991: Determination of the optical thickness and effective particle radius of clouds from reflected solar radiation measurements. Part II: Marine stratocumulus observations. *J. Atmos. Sci.,* **48,** 728–750.

Platnick, S., and S. Twomey, 1994: Determining the susceptibility of cloud albedo to changes in droplet concentration with the Advanced Very High Resolution Radiometer. *J. Appl. Meteor.,* **33,** 334–347.

Radke, L. F., J. A. Coakley Jr., and M. D. King, 1989: Direct and remote sensing observations of the effects of ships on clouds. *Science,* **246,** 1146–1149.

Rawlins, F., and J. S. Foot, 1990: Remotely sensed measurements of stratocumulus properties during FIRE using the C130 aircraft multi-channel radiometer. *J. Atmos. Sci.,* **47,** 2488–2503.

Rossow, W. B., 1978: Cloud microphysics: Analysis of the clouds of Earth, Venus, Mars and Jupiter. *Icarus,* **36,** 1–50.

——, L. C. Garder, and A. A. Lacis, 1989: Global, seasonal cloud variations from satellite radiance measurements. Part I: Sensitivity of analysis. *J. Climate,* **2,** 419–458.

——, ——, P. J. Lu, and A. W. Walker, 1991: International Satellite Cloud Climatology Project (ISCCP) documentation of cloud data. WMO/TD-No. 266, World Meteor. Org., 76 pp. plus 3 appendices.

Schwartz, S. E., 1988: Are global cloud albedo and climate controlled by marine phytoplankton? *Nature,* **336,** 441–445.

——, and M. O. Andreae, 1996: Uncertainty in climate change caused by aerosols. *Science,* **272,** 1121–1122.

——, and A. Slingo, 1996: Enhanced shortwave cloud radiative forcing due to anthropogenic aerosols. *Clouds, Chemistry and Climate,* P. J. Crutzen and V. Ramanathan, Eds., NATO ASI Series, Vol. 135, Springer–Verlag, 191–235.

Slingo, A., 1988: Can plankton control climate? *Nature,* **336,** 421.

——, 1990: Sensitivity of the Earth's radiation budget to changes in low clouds. *Nature,* **343,** 49–51.

Smith, R. N. B., 1990: A scheme for predicting layer clouds and their water content in a general circulation model. *Quart. J. Roy. Meteor. Soc.,* **116,** 435–460.

Stephens, G. L., 1978: Radiation profiles in extended water clouds. Part II: Parameterization schemes. *J. Atmos. Sci.,* **35,** 2123–2132.

Tiedtke, M., 1993: Representation of clouds in large-scale models. *Mon. Wea. Rev.,* **121,** 3040–3061.

Twohy, C. H., P. A. Durkee, R. J. Huebert, and R. J. Charlson, 1995: Effects of aerosol particles on the microphysics of coastal stratiform clouds. *J. Climate,* **8,** 773–783.

Twomey, S., 1977: The influence of pollution on the shortwave albedo of clouds. *J. Atmos. Sci.,* **34,** 1149–1152.

——, 1991: Aerosols, clouds and radiation. *Atmos. Environ.,* **25A,** 2435–2442.

——, M. Piepgrass, and T. L. Wolfe, 1984: An assessment of the impact of pollution on global cloud albedo. *Tellus,* **36B,** 356–366.

Wielicki, B. A., and L. Parker, 1992: On the determination of cloud cover from satellite sensors: The effect of sensor spatial resolution. *J. Geophys. Res.,* **97,** 12 799–12 823.